




# Assessing Analytical and Functional Similarity of Proposed Amgen Biosimilar ABP 980 to Trastuzumab

Katariina M. Hutterer<sup>1</sup> · Alla Polozova<sup>2</sup> · Scott Kuhns<sup>1</sup> · Helen J. McBride<sup>1</sup>  · Xingxiang Cao<sup>1</sup> · Jennifer Liu<sup>1</sup>

Published online: 10 April 2019  
© The Author(s) 2019

## Abstract

**Background** ABP 980 has been developed as a biosimilar to Herceptin<sup>®</sup> (trastuzumab). Comprehensive analytical characterization incorporating orthogonal analytical techniques was used to compare ABP 980 to trastuzumab reference products sourced from the United States (US) and the European Union (EU).

**Methods** Physicochemical property comparisons included the following: primary structure related to amino acid sequence and post-translational modifications, including glycans; higher-order structure; product-related substances and impurities, including size and charge variants; subvisible and submicron particles, and protein content. In addition, functional similarity was assessed for Fab-mediated, Fc-mediated, and combined Fab- and Fc-mediated activities.

**Results** ABP 980 has the same amino acid sequence as and similar post-translational modification profiles to trastuzumab (US) and trastuzumab (EU). Importantly, ABP 980 was found to be highly similar to trastuzumab for all functional activities related to the mechanism(s) of action. Higher-order structure, product-related substances and impurities, particles and aggregates were also highly similar between ABP 980 and trastuzumab. Where minor differences were noted, they were evaluated and found unlikely to impact clinical performance. The totality of evidence, including the pharmacokinetic clinical similarity of ABP 980, further supports that ABP 980 is highly similar to trastuzumab.

**Conclusion** Based on the comprehensive analytical similarity assessment, ABP 980 is analytically highly similar to the reference product, trastuzumab.

## Key Points

ABP 980 was found to be highly similar to trastuzumab for all functional activities related to the mechanism(s) of action.

Higher-order structure, product-related substances and impurities, particles and aggregate were highly similar between ABP 980 and trastuzumab.

## 1 Introduction

Herceptin<sup>®</sup> (trastuzumab) is approved for use in the United States (US), European Union (EU), and much of the rest of the world for treatment of metastatic breast cancer, early breast

cancer, and metastatic gastric cancer [1, 2], and is the standard of care for patients with human epidermal growth factor receptor 2 (HER2)-overexpressing breast cancer [3–5]. Trastuzumab binds to the extracellular domain (ECD) of HER2, blocking receptor activation and subsequent proliferation of cells that express HER2, and induces antibody-dependent cellular cytotoxicity (ADCC) and antibody-dependent cellular phagocytosis (ADCP) on HER2-expressing cells [6]. ABP 980 is being developed by Amgen Inc. as a biosimilar to trastuzumab. ABP 980 and trastuzumab are immunoglobulin G type 1 (IgG1) monoclonal antibodies (mAbs) expressed in Chinese hamster ovary (CHO) cells.

Biosimilars are produced in different cell lines (i.e., from a different transfection event) and have different manufacturing processes to the reference product. Therefore, minor structural and functional differences between biosimilars and the reference product are unavoidable due to their complex molecular structure and the unique, often proprietary, manufacturing processes involved in their production. Consequently, it is not possible to produce biosimilar molecules that are identical to the reference product [7]. Nevertheless, each biosimilar must demonstrate similarity to the reference product. To meet this challenge, the US Food and Drug Administration (FDA) and

✉ Katariina M. Hutterer  
hutterer@amgen.com

<sup>1</sup> Amgen Inc., One Amgen Center Drive, Thousand Oaks, CA 91320, USA

<sup>2</sup> Amgen Inc., 360 Binney Street, Cambridge, MA 02142, USA

European Medicines Agency (EMA) have published guidance for the stepwise development of biosimilars. The foundation of the stepwise approach is demonstrating structural and functional similarity [8]. Sensitive analytical methods capable of detecting structural and functional differences are the foundation of the stepwise biosimilar evaluation process, and any differences that are identified are further evaluated to confirm they do not affect clinical efficacy and safety [9–11]. Additionally, ABP 980 has been shown to be similar to trastuzumab in non-clinical xenograft models and a phase 1 pharmacokinetic (PK) study in healthy volunteers [12, 13]. Further, results from a phase 3 clinical study have confirmed similar efficacy and safety between ABP 980 and trastuzumab when treating patients with early breast cancer [14].

A comprehensive analytical and functional assessment of the proposed biosimilar ABP 980 was conducted to determine its similarity to FDA-licensed trastuzumab (trastuzumab [US]) and EU-authorized trastuzumab (trastuzumab [EU]). This analysis included lots manufactured from all drug substance lots used in the clinical trials. ABP 980 lots were compared to 23 lots of trastuzumab (US) and 33 lots of trastuzumab (EU), which were procured over a period of approximately 5 years. The methods used for the analytical similarity assessment were selected based on knowledge regarding the structure and function of ABP 980 and trastuzumab, focusing on those characteristics critical to biological activity, including HER2 binding, potency as measured by ligand-independent inhibition of proliferation, and ADCC. The similarity assessment strategy was designed to comprehensively assess structure and functional attributes compared to pre-defined assessment criteria, to ensure that any differences between ABP 980 and trastuzumab were identified and evaluated in line with US and EU regulatory guidelines. The results presented here are numeric results, along with representative profiles, demonstrating the similarity of ABP 980 to the reference product, trastuzumab.

## 2 Materials and Methods

ABP 980 was developed by Amgen as a biosimilar to Herceptin® (trastuzumab). Multiple lots of trastuzumab from US and EU regions were procured over a period of approximately 5 years. The expiration dates for the trastuzumab lots ranged from February 2015 to March 2020. All analyses were performed at Amgen except where noted. The lots included for the similarity assessment of each parameter were based on the impact of the process on that parameter. For parameters primarily influenced by the drug substance manufacturing process (e.g., glycan profile, biological functions), only a single drug product lot for each independent drug substance was included. When a drug product lot was not available, the drug substance lot was included for these parameters. For parameters primarily influenced by the drug product manufacturing

process (e.g., protein content, reconstitution time), data from all available drug product lots were included.

### 2.1 Product Strength: Protein Content and Reconstituted Protein Concentration

Samples were reconstituted then gravimetrically diluted, and the protein concentration of each vial was determined using the ultraviolet (UV) absorbance, the dilution factor, and the theoretical protein extinction coefficient [15]. The product volume of each vial was determined gravimetrically, correcting for density. The protein content of each vial was the product of the protein concentration and the product volume.

### 2.2 Peptide Mapping

A single replicate of each sample was reduced with dithiothreitol (DTT) in denaturant and alkylated with sodium iodoacetate. Excess reagents were removed by gel-filtration desalting spin columns. Subsequently, samples were digested with trypsin for 35 min at 37 °C. The resulting peptides were separated by reversed-phase (RP) ultra high-performance liquid chromatography (UHPLC) in a trifluoroacetic acid (TFA)/acetonitrile (ACN) gradient, monitored by UV at 214 nm and mass spectrometry (MS).

### 2.3 Whole Mass

The intact molecular mass of ABP 980 and trastuzumab (EU) was determined by electrospray ionization–time of flight–mass spectrometer (ESI–TOF–MS) analysis. Single replicates of samples were separated from buffer components and introduced to the mass spectrometer by high-performance liquid chromatography (HPLC). The resulting ion spectra were deconvoluted to produce molecular mass profiles. The theoretical mass calculations assume that all of the disulfide bonds are intact and there are no C-terminal lysine residues on the heavy chain (HC) of trastuzumab.

### 2.4 N-Glycan Mapping

The N-linked glycan profiles of samples were evaluated by hydrophilic interaction liquid chromatography (HILIC) UHPLC glycan map analysis. N-linked glycans were released from the protein backbone using peptide-N-glycosidase F (PNGase F) of a single replicate. The released glycans were derivatized with the fluorescent label 2-aminobenzoic acid at the reducing terminal N-acetylglucosamine (GlcNAc). Fluorescently labeled oligosaccharides were separated by HILIC. Bound oligosaccharides were eluted,

and relative percent peak areas of the oligosaccharides were calculated.

## 2.5 Size Variants by Size-Exclusion Ultra high-Performance Liquid Chromatography (SE-UHPLC)

Size-exclusion ultra high-performance liquid chromatography (SE-UHPLC) was used to quantify levels of individual size variants, such as high molecular weight (HMW) species, low molecular weight (LMW) species, and main peak. The single replicate samples were loaded onto an SE-UHPLC column, separated isocratically, and the eluent was monitored by UV absorbance.

## 2.6 Secondary Structure by Fourier-Transformed Infrared Spectroscopy (FTIR)

Secondary structure was assessed by Fourier-transformed infrared spectroscopy (FTIR). Single replicate FTIR measurements were made at room temperature using a Bruker Vertex 70 FTIR spectrometer (Bruker Corporation, Billerica, MA). The spectrum of the buffer blank was recorded under identical conditions and was subtracted from the protein spectrum. The second derivative spectrum was calculated using a 9-point smoothing of the original spectrum. Spectral similarity was quantitatively determined using the Thermo OMNIC software QC compare function (Thermo Scientific).

## 2.7 Tertiary Structure by Near Ultraviolet-Circular Dichroism (UV CD) Spectroscopy

Tertiary structure was assessed by near ultraviolet-circular dichroism (UV CD) spectroscopy. Single replicate near UV CD measurements were made on an Applied Photophysics Chirascan spectropolarimeter (Applied Photophysics Ltd, Leatherhead, United Kingdom) at ambient temperature using cuvettes with a path length of 1 cm. All drug product samples were diluted to approximately 0.7 mg/mL with product buffer prior to measurements. The resulting spectra were corrected for protein concentration and contributions from buffer, and reported as circular dichroism ellipticity. Spectral similarity was quantitatively determined using the Thermo OMNIC software QC compare function (Thermo Scientific).

## 2.8 Thermal Stability by Differential Scanning Calorimetry (DSC)

Thermal stability was assessed by differential scanning calorimetry (DSC). DSC measurements were made in

triplicate using a MicroCal VP-Capillary DSC system (GE Healthcare Bio-Sciences, Pittsburgh, PA). All samples were diluted to approximately 1 mg/mL with product buffer prior to measurements.

## 2.9 Subvisible Particles by Light Obscuration (LO) and Micro-Flow Imaging (MFI)

Subvisible particles were assessed by light obscuration (LO). Single replicate LO measurements were made with an HIAC 9703 + liquid particle counting system (Beckman Coulter Life Sciences; Brea, CA) equipped with an HRLD 150 sensor. For each sample test, the particle concentration results were reported as cumulative particle counts/mL.

Subvisible particles were further assessed by micro-flow imaging (MFI). Single replicate MFI measurements were made with an MFI 5200 system equipped with a 100  $\mu\text{m}$ /1.6 mm/SP3 flow cell (ProteinSimple, San Jose, CA). For each sample test, particle concentration results were reported as cumulative particle counts/mL of  $\geq 5 \mu\text{m}$  non-spherical particles with an aspect ratio of  $< 0.85$ .

## 2.10 Aggregates by Sedimentation Velocity Analytical Ultracentrifugation (SV-AUC)

Aggregates were analyzed by sedimentation velocity analytical ultracentrifugation (SV-AUC). Triplicate SV-AUC measurements were made at 45,000 rpm following UV absorbance at 280 nm. All product samples were diluted to approximately 0.5 mg/mL with product buffer before measurements. Scans were collected at 20 °C without delay between them. Data were analyzed allowing the frictional ratio, time invariant noise, and meniscus values to float during the non-linear least squares fit.

## 2.11 Aggregates by Size-Exclusion High-Performance Liquid Chromatography (SE-HPLC) coupled with Light Scattering (LS) Detection

Aggregates were analyzed by size-exclusion high-performance liquid chromatography–light scattering (SE-HPLC–LS). Triplicate samples without dilution were injected into the HPLC system, and the molecular weights were calculated for monomer and HMW species.

## 2.12 Fc Neonatal Receptor (FcRn) Binding

A two-step AlphaScreen<sup>®</sup> (Perkin Elmer, Shelton, CT, USA) receptor binding assay was used to quantify the binding of human IgG Fc domain and Fc neonatal receptor (FcRn). The assay measured the dose-dependent signal decrease observed when an Fc-containing sample is added to a

reaction containing FcRn-His (Amgen, Inc. Thousand Oaks, CA, USA) and Fc-biotin (Amgen, Inc. Thousand Oaks, CA, USA). When ABP 980 or trastuzumab is present at sufficient concentrations to inhibit the binding of FcRn to the biotinylated human Fc, a dose-dependent decrease in emission is measured using a plate reader. Activity was determined by comparing the sample response to the response obtained for the reference standard. The sample binding relative to the reference standard was determined using a four-parameter logistic model fit (SoftMax<sup>®</sup> Pro Software, Molecular Devices, Sunnyvale, CA, USA). Each sample was tested in three independent assays, and the final valid result for a given sample was reported as the mean of the three measurements. Results were reported as percentage relative binding values.

### 2.13 Fc gamma Receptor Type 2a (FcγRIIa) and FcγRIIIa Binding

Relative binding to Fc gamma receptor type 2a (FcγRIIa) (131H), FcγRIIIa (158 V), and FcγRIIIa (158F) was quantified using AlphaLISA<sup>®</sup> assays (Perkin Elmer, Shelton, CT, USA). Recombinant, purified human FcγRIIa (131H), FcγRIIIa (158 V) and FcγRIIIa (158F) glutathione S-transferase (GST)-fusion proteins were generated at Amgen Inc. Thousand Oaks, CA, USA through either a CHO or 293 cell expression system. The AlphaLISA<sup>®</sup> assay is an Amplified Luminescent Proximity Homogenous Assay (Alpha) designed to measure the level of Fc gamma receptor (FcγR) binding to the Fc portion of IgG1 mAbs. The assay contained two bead types, an acceptor bead and a donor bead. The acceptor bead is coated with glutathione and binds recombinant human FcγR-GST. The donor beads are coated with streptavidin, which binds to biotinylated human IgG1 (Amgen Inc. Thousand Oaks, CA, USA). When trastuzumab or ABP 980 is present at sufficient concentrations to inhibit the binding of FcγR-GST to the biotinylated human IgG1, a dose-dependent decrease in emission is measured using a plate reader. The sample binding relative to the reference standard was determined using a four-parameter logistic model fit (SoftMax<sup>®</sup> Pro Software, Molecular Devices, Sunnyvale, CA, USA). Each sample was tested in three independent assays, and the final valid result for a given sample was reported as the mean of the three measurements. Results were reported as percentage relative binding values for FcγRIIa (131H), FcγRIIIa (158 V) or FcγRIIIa (158F).

### 2.14 Human Epidermal Growth Factor Receptor 2 (HER2) Binding Enzyme-Linked Immunosorbent Assay (ELISA)

A solid-phase enzyme-linked immunosorbent assay (ELISA) was used to determine the binding of human HER2 to ABP

980 and trastuzumab. Recombinant human HER2 (rHER2) (AcroBiosystems, Newark, DE, USA) was coated onto the wells of a microtiter ELISA plate. After washing the wells to remove unbound protein, the remaining uncoated portions of the plate were blocked using a blocking buffer. Plates were then washed and a serial dilution of reference standard, control and sample(s) was added to the appropriate wells and incubated. Wells were again washed and goat anti-human IgG (Fc fragment) conjugated to horseradish peroxidase (HRP) (ThermoFisher, Waltham, MA, USA) was added. After a final wash, a peroxidase substrate/chromogen solution was added to the wells. The substrate changes color in the presence of HRP, in proportion to the amount of ABP 980 or trastuzumab bound to HER2 by the samples and standard. The reaction was stopped with 1.0 M phosphoric acid, and absorbance was measured with a microplate reader. The test-sample binding relative to the reference standard was determined using a four-parameter logistic model fit (SoftMax<sup>®</sup> Pro Software, Molecular Devices, Sunnyvale, CA, USA). Each sample was tested in three independent assays, and the final valid result for a given sample was reported as the mean of the three measurements. Results were reported as percentage relative binding values.

### 2.15 Inhibition of Proliferation in BT-474 Cells

BT-474 cells were incubated with varying concentrations of reference standard, assay control, and samples. After a timed incubation, Cell-Titer Glo<sup>®</sup> Luminescent Cell Viability Assay Reagent (Promega, Madison, WI, USA) system was added to the assay plates. Addition of Cell-Titer Glo<sup>®</sup> reagent results in cell lysis and generation of luminescence signal, which is proportional to the amount of adenosine triphosphate (ATP) present. The amount of ATP present was directly proportional to the number of viable cells in the culture and inversely proportional to the concentration of ABP 980 or trastuzumab. The test-sample bioactivity relative to the reference standard was determined using a four-parameter logistic model fit. Each sample was tested in three independent assays, and the final valid result for a given sample was reported as the mean of the three measurements. Results were reported as percentage relative potency.

### 2.16 NK92 Antibody-Dependent Cellular Cytotoxicity (ADCC) Assay

To assess ADCC, HCC2218 cells that overexpress HER2 receptors were used as target cells, and NK92-M1 cells, stably transfected with human FcγRIIIa (158 V), were used as effector cells. Target cells were loaded with calcein-AM (Sigma-Aldrich, St. Louis, MO, USA). ADCC activity was assessed by adding effector cells to the opsonized target cells at an effector-to-target ratio of 25:1 and incubated for

approximately 1 h. Calcein released from lysed target cells was determined by measuring the fluorescence of the supernatant. Each sample was tested in three independent assays, and the final valid result for a given sample was reported as the mean of the three measurements. The test-sample bioactivity relative to the reference standard was determined using a four-parameter logistic model fit (SoftMax<sup>®</sup> Pro Software, Molecular Devices, Sunnyvale, CA, USA). Results were reported as percentage relative NK92 ADCC.

### 2.17 Peripheral Blood Mononuclear Cell (PBMC) ADCC Assay

Peripheral blood mononuclear cells (PBMC) isolated from FcγRIIIa-158 V/F heterozygous donors were used as effector cells. SKBR3 HER2-expressing breast cancer cells were used as target cells in the assay. Target and effector cells were incubated with test samples for 18–24 h. After incubation, CytoTox Glo<sup>®</sup> Cytotoxicity Assay Reagent was added to the assay plates. CytoTox Glo<sup>®</sup> measures the presence of intracellular protease activity (dead-cell protease) that is released from membrane-compromised cells. The quantity of dead-cell protease in the medium, and thus luminescence, is directly proportional to the number of dead cells in the culture. Each sample was tested in three independent assays, and the final valid result for a given sample was reported as the mean of the three measurements. The test-sample bioactivity relative to the reference standard was determined using a four-parameter logistic model fit (PLA 2 Software, Steggmann Systems GmbH, Rodgau, Germany). Results were reported as percentage relative PBMC ADCC.

## 3 Results

The similarity testing plan and analytical methods used for the physicochemical and functional characterization of ABP 980 and trastuzumab are summarized in Table 1. Results of key structural and function characterization tests are presented here.

### 3.1 Primary Structure

The primary structures of ABP 980 and trastuzumab were investigated by several complementary characterization methods, including intact mass, reduced and deglycosylated HC and light chain (LC) mass analysis, peptide mapping, and glycan map. Results of the intact mass and reduced and deglycosylated HC and LC mass analyses are summarized in Table 2. The results showed ABP 980 and trastuzumab have the same molecular mass, which is also consistent with the theoretical mass. Reduced peptide map overlays are displayed in Fig. 1a. The chromatograms for the three

products are visually similar; no new or missing peaks were identified. In addition, the same N-linked glycosylation site at N<sup>300</sup> was detected in the same glycopeptide in ABP 980 and trastuzumab. These results demonstrate that ABP 980 and trastuzumab have the same amino acid sequences.

The glycan profile of mAbs, specifically levels of afucosylated, galactosylated, and high mannose species, can influence binding to the FcγRIIIa receptor, which mediates ADCC activity. The percentage values of individual glycan species and glycan groups and glycan map profiles for representative lots of ABP 980, trastuzumab (US), and trastuzumab (EU) are shown in Table 2 and Fig. 1b. Although the abundance of certain individual glycan species, such as A1G0F, differ, similar levels of the key glycan groups—afucosylated, galactosylated, sialylated, and high mannose species—were present in ABP 980 compared to trastuzumab. However, the ranges for afucosylated and galactosylated species for trastuzumab (US) and trastuzumab (EU) are fairly wide. These combinations of glycans species, particularly the afucosylated and galactosylated species, influence binding to FcγRIIIa and ADCC activity, as shown in Fig. 2. This figure shows predicted NK92 ADCC, a formula for which was derived using JMP statistical software by determining which product quality attributes had a statistically significant impact on the measured NK92 ADCC. Then, the leverage of each statistically significant factor was determined to compute the predicted NK92 ADCC for any given glycan combination. High mannose, up to a level of 5%, was not found to have a significant impact on binding to FcγRIIIa and ADCC activity (Fig. 2d) ( $p$  value = 0.5505). All three products, ABP 980, trastuzumab (US), and trastuzumab (EU), follow the same glycan–ADCC relationship, as illustrated by the combined data set shown in Fig. 2. No new peaks were observed in the ABP 980 glycan map compared with trastuzumab.

### 3.2 Higher-Order Structure

ABP 980 and trastuzumab were characterized by FTIR for secondary structure, by near UV CD for tertiary structure, and by DSC for thermal stability. The results are shown in Table 2 and Fig. 3. The FTIR profiles of ABP 980 and trastuzumab are visually similar, with peaks at around 1639 cm<sup>-1</sup> and 1689 cm<sup>-1</sup>, indicating the presence of a predominantly antiparallel beta-sheet structure typical of antibodies. The spectral similarity analysis demonstrates that the FTIR spectra are ≥ 95% similar. The near UV CD profiles of ABP 980 and trastuzumab are visually similar with peaks corresponding to optical activities of tryptophan, tyrosine, and phenylalanine, superimposed on the broad disulfide signal from 250 to 320 nm. The intensity of these features reflects the native structure and demonstrates that the disulfide bonds and aromatic amino acids are in the expected environment due to the proper folding of the proteins. The spectral

**Table 1** Attributes and analytical techniques for characterization of ABP 980 and trastuzumab reference product

Category	Analytical techniques and attributes
Primary structure	Whole mass by mass spectrometry: intact molecular mass and mass spectrum profile Reduced and deglycosylated molecular masses of HC and LC: molecular masses of HC and LC and mass spectrum profile Reduced peptide map: amino acid sequence, peptide map profile, post-translational modifications Non-reduced peptide map: disulfide structure and peptide map profile Glycan map by HILIC HPLC: afucosylation, high mannose, galactosylation, afucosylated galactosylation, sialylation, glycan map profile cIEF: isoelectric point, profile Amino acid analysis: extinction coefficient Identity by ELISA
Higher-order structure	FTIR: spectral similarity, spectral profile Near UV CD: spectral similarity, spectral profile DSC: $T_{m1}$ , $T_{m2}$ , profile
Particles and aggregates	HIAC: $\geq 2 \mu\text{m}$ , $\geq 5 \mu\text{m}$ , $\geq 10 \mu\text{m}$ , $\geq 25 \mu\text{m}$ particles MFI: $\geq 5 \mu\text{m}$ particles and $\geq 5 \mu\text{m}$ non-spherical particles SV-AUC: HMW, profile SE-HPLC-LS: Molar mass, profile
Product-related substances and impurities	SE-UHPLC: HMW, main peak, LMW, profile rCE-SDS: HC + LC, LMW + MMW, NGHC, profile nrCE-SDS: pre-peaks, main peak, profile
Thermal stability and degradation	SE-HPLC: HMW, main peak degradation rCE-SDS: HC + LC, LMW + MMW, NGHC degradation nrCE-SDS: pre-peak degradation Proliferation inhibition bioassay: potency degradation
General properties	Protein content: protein content, reconstituted protein concentration Reconstitution time
Process-related impurities	HCP ELISA 2D-DIGE LC/MS Protein A ELISA qPCR
Fab-mediated biological activity	Potency: proliferation inhibition (BT-474 cells) HER2 binding: ELISA, SPR Inhibition of AKT phosphorylation Proliferation inhibition (NCI-N87 cells) Proliferation inhibition synergy with chemotherapeutic (NCI-N87 cells) Lack of proliferation inhibition (non-amplified HER2 MCF7 cells)
Fc-mediated biological activity	FcRn binding FcγRIIIa (158 V) binding FcγRIIIa (158F) binding FcγRIa binding FcγRIIa (131H) binding FcγRIIb binding FcγR binding on primary macrophages FcγRIIb binding C1q binding
Fab and Fc-mediated biological activity	NK92 ADCC activity PBMC ADCC activity Lack of ADCC (HER2-negative cells) ADCP activity Lack of CDC activity

*2D-DIGE* two-dimensional differential in-gel electrophoresis, *ADCC* antibody-dependent cellular cytotoxicity, *ADCP* antibody-dependent cellular phagocytosis, *CDC* complement-dependent cytotoxicity, *cIEF* capillary isoelectric focusing, *DSC* differential scanning calorimetry, *ELISA* enzyme-linked immunosorbent assay, *FcγR* Fc gamma receptor, *FcγRIa* Fc gamma receptor type 1a, *FcγRIIa* Fc gamma receptor type 2a, *FcγRIIb* Fc gamma receptor type 2b, *FcγRIIIa* Fc gamma receptor type 3a, *FcRn* Fc neonatal receptor, *FTIR* Fourier-transformed infrared, *HC* heavy chain, *HER2* human epidermal growth factor receptor 2, *HILIC* hydrophilic interaction liquid chromatography, *HMW* high molecular weight, *HPLC* high-performance liquid chromatography, *LC* light chain, *LC/MS* liquid chromatography with mass spectrometry, *LMW* low molecular weight, *MFI* micro-flow imaging, *NGHC* non-glycosylated heavy chain, *nrCE-SDS* non-reduced capillary electrophoresis with sodium dodecyl sulfate, *PBMC* peripheral blood mononuclear cells, *qPCR* quantitative polymerase chain, *reactionnrCE-SDS* reduced capillary electrophoresis with sodium dodecyl sulfate, *SDS* sodium dodecyl sulfate, *SE-HPLC-LS* size-exclusion high-pressure liquid chromatography-light scattering, *SE-UHPLC* size-exclusion ultra high-performance liquid chromatography, *SPR* surface plasmon resonance, *SV-AUC* sedimentation velocity analytical ultracentrifugation, *UV CD* ultraviolet circular dichroism

**Table 2** Summary of structural attributes for ABP 980, trastuzumab (US), and trastuzumab (EU)

Attribute	ABP 980 Range (n)	Trastuzumab (US) Range (n)	Trastuzumab (EU) Range (n)
Intact molecular weight, difference between observed and theoretical (ppm)			
Glycosylation: A2G0F:A2G0F	37–42 (4)	28–43 (3)	28–33 (3)
Glycosylation: A2G0F:A2G1F	22–28 (4)	19–23 (3)	19–20 (3)
Glycosylation: A2G1F:A2G1F, A2G0F:A2G2F	22–25 (4)	18–19 (3)	15–20 (3)
Glycosylation: A2G1F:A2G2F	25–31 (4)	17–21 (3)	19–25 (3)
Reduced and deglycosylated light chain, difference between observed and theoretical (ppm)	35–37 (4)	36–37 (3)	36–36 (3)
Reduced and deglycosylated heavy chain, difference between observed and theoretical (ppm)	20–22 (4)	21–22 (3)	21–22 (3)
Glycan profile (%)			
Galactosylation	42.7–57.0 (22)	21.8–53.4 (23)	22.0–51.4 (33)
High mannose	1.5–4.2 (22)	2.1–6.5 (23)	1.8–4.8 (33)
Afucosylation	7.6–9.1 (22)	5.1–8.6 (23)	5.1–9.2 (33)
Sialylation	0.8–1.7 (22)	1.2–2.4 (23)	1.1–2.6 (33)
Glycosylation at Asn300 (%) (n)	99.3–99.8 (13)	98.6–99.1 (21)	98.5–99.2 (33)
FTIR: spectral similarity, relative to trastuzumab (US), (%)	99.5–100.0 (7)	99.4–100.0 (6)	99.3–100.0 (6)
Near UV CD: spectral similarity, relative to trastuzumab (US) (%)	98.1–99.2 (7)	98.5–100 (6)	97.1–99.4 (6)
DSC: $T_{m1}$ (°C)	70.6–70.9 (11)	70.7–71.0 (9)	70.7–71.0 (9)
DSC: $T_{m2}$ (°C)	82.5–82.7 (11)	82.5–82.6 (9)	82.5–82.6 (9)
LO: $\geq 2$ - $\mu\text{m}$ particles/mL	8–1466 (6)	64–361 (30)	102–534 (6)
LO: $\geq 5$ - $\mu\text{m}$ particles/mL	1–237 (30)	10–45 (6)	6–28 (6)
LO: $\geq 10$ - $\mu\text{m}$ particles/mL	0–40 (30)	1–9 (6)	1–4 (6)
LO: $\geq 25$ - $\mu\text{m}$ particles/mL	0–8 (30)	0–2 (6)	0–1 (6)
MFI: $\geq 5$ - $\mu\text{m}$ particles/mL	0–100 (28)	72–414 (6)	50–144 (6)
MFI: $\geq 5$ - $\mu\text{m}$ non-spherical particles/mL	0–52 (28)	64–330 (6)	26–108 (6)
SV-AUC: HMW	< LOQ	< LOQ	< LOQ
SE-HPLC–LS: molar mass of monomer (kDa)	144–148 (7)	144–148 (6)	143–148 (6)
SE-HPLC–LS: molar mass of pre-peak (kDa)	281–318 (7)	283–313 (6)	281–314 (6)
Protein content (mg/vial)			
ABP 980 (440-mg presentation) vs trastuzumab (US) (n)	422–441 (7)	424–447 (21)	–
ABP 980 (150-mg presentation) vs trastuzumab (EU) (n)	148–157 (22)	–	150–159 (30)
Protein concentration in mg/mL (n)	20.0–21.4 (29)	20.6–21.6 (20)	20.4–21.3 (30)

DSC differential scanning calorimetry, FTIR Fourier-transformed infrared, HMW high molecular weight, LO light obscuration, LOQ limits of quantitation, MFI micro-flow imaging, n number of lots analyzed, SE-HPLC–LS size-exclusion high-pressure liquid chromatography–light scattering, SV-AUC sedimentation velocity analytical ultracentrifugation, trastuzumab (EU) European Union-authorized trastuzumab, trastuzumab (US) United States Food and Drug Administration-licensed trastuzumab, UV CD ultraviolet circular dichroism

similarity analysis demonstrates that the near UV CD spectra are  $\geq 95\%$  similar. The DSC results show that the thermal transition temperatures are similar between ABP 980 and trastuzumab. Taken together, these results indicate that ABP 980 has similar higher-order structures to trastuzumab.

### 3.3 Particles and Aggregates

Particles and aggregates of ABP 980 and trastuzumab were assessed using a combination of test methods capable of detecting the presence and/or quantifying the amounts of particles and aggregates of various sizes and shapes

(spherical or non-spherical) with a focus on proteinaceous particles. Subvisible particles were evaluated quantitatively by LO and characterized by MFI for morphology, specifically the presence of non-spherical particles, which could be proteinaceous, as opposed to spherical particles often corresponding to silicone oil droplets. Particle concentrations for  $\geq 2$ -,  $\geq 5$ -,  $\geq 10$ -, and  $\geq 25$ - $\mu\text{m}$  sizes are shown in Table 2. The subvisible particles, as characterized by LO and MFI, show ABP 980 and trastuzumab products have low and similar amounts of subvisible particles in the  $\geq 2$ -,  $\geq 5$ -,  $\geq 10$ -, and  $\geq 25$ - $\mu\text{m}$  sizes, and similar amounts of non-spherical particles in the  $\geq 5$ - $\mu\text{m}$  size range.

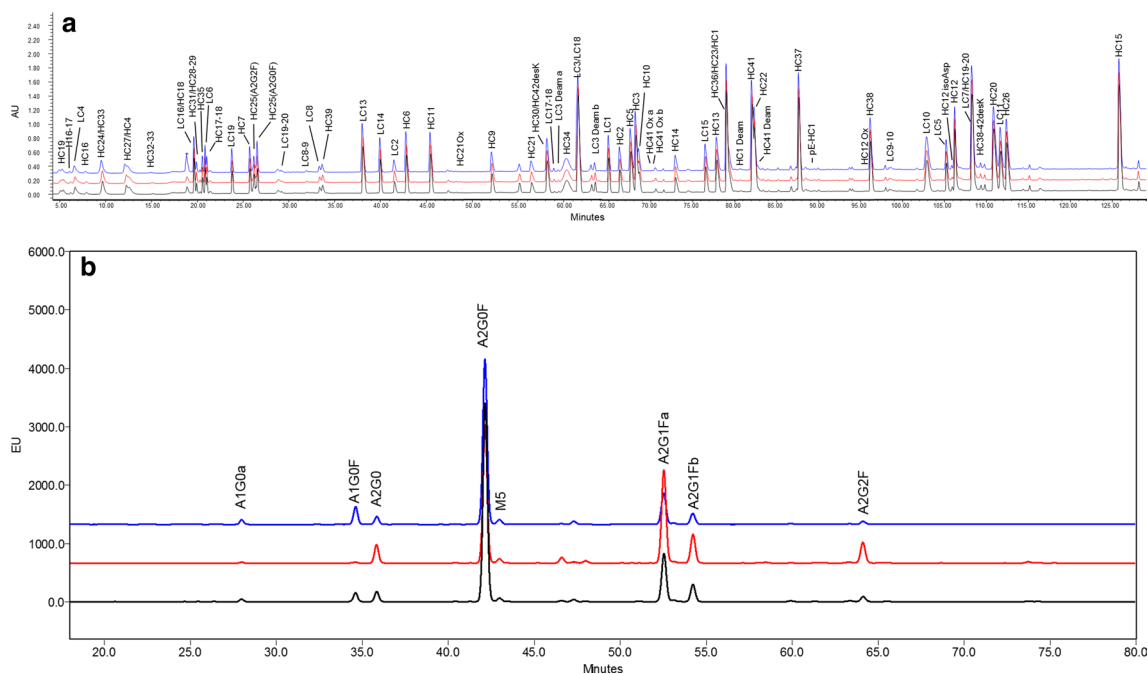


**Fig. 1** Primary structure comparisons of trastuzumab (EU) (top, blue line), ABP 980 (middle, red line), and trastuzumab (US) (bottom, black line): **a** peptide map and **b** glycan map

Soluble aggregates were characterized by SE-HPLC–LS and SV-AUC. The molecular weight of aggregates detected by SE-HPLC–LS was consistent with dimers. Aggregates detected by SV-AUC were below the limits of quantitation (LOQ) for all products, as shown in Table 2. Characterization by SE-HPLC–LS and SV-AUC shows that aggregates in ABP 980 and trastuzumab products are similar in size and level.

### 3.4 Size Variants

SE-UHPLC is used to quantify levels of individual size variants, such as HMW, LMW, and main peak. The SE-UHPLC profiles of ABP 980, trastuzumab (US), and trastuzumab (EU) are visually similar across the three products, with minor differences in the HMW and LMW regions (Fig. 4). Levels of HMW and LMW for all three products are very low, the HMW has been characterized as dimer, and the LMW levels of all three products are close to the LOQ (0.1%) of the method.

The non-reduced capillary electrophoresis with sodium dodecyl sulfate (nrCE-SDS) method is used to quantify size variants under non-reduced, but denaturing conditions. This allows for the detection of both partially reduced species and fragments (clips) in the “pre-peaks.” The nrCE-SDS profiles of ABP 980, trastuzumab (US), and trastuzumab (EU) are visually similar across the three products.

The reduced capillary electrophoresis with sodium dodecyl sulfate (rCE-SDS) method is used to quantify size

variants such as non-glycosylated heavy chain (NGHC), clips [low molecular weight and mid-molecular weight (LMW + MMW)], and purity (LC + HC). The rCE-SDS profiles of ABP 980, trastuzumab (US), and trastuzumab (EU) are visually similar across the three products, with minor differences in the NGHC levels. The slightly lower level of NGHC in ABP 980 does not impact biological activity, as demonstrated by the functional activity of ABP 980 across the panel of biological assays tested.

### 3.5 Protein Content and Concentration

Protein content for the 440-mg presentation (vs trastuzumab [US]) and the 150-mg presentation (vs trastuzumab [EU]) and protein concentration are similar (Table 2).

Overall, the evidence suggests ABP 980, trastuzumab (US), and trastuzumab (EU) are similar with respect to physicochemical properties, with only minor quantitative differences that did not influence functional parameters and are not expected to be clinically meaningful.

### 3.6 HER2 Binding

Uncontrolled ligand-independent activation of HER2 can lead to increased survival and proliferation of tumor cells. There is a strong positive correlation between HER2 over-expression and breast tumor aggressiveness, and a negative correlation with patient outcomes. By binding to HER2,



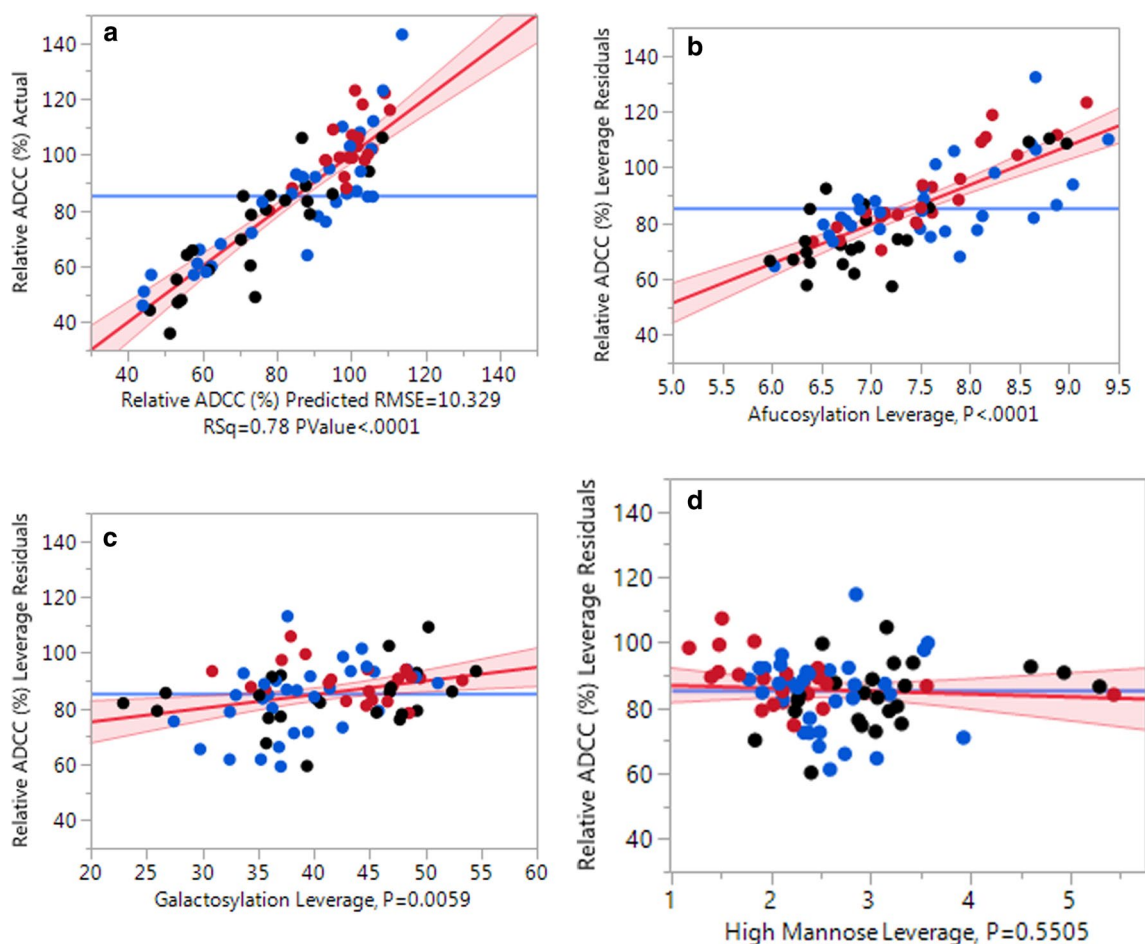


**Fig. 2** Correlation of NK92 ADCC with glycan composition: **a** overall structure–function model; **b** relative contribution of afucosylation; **c** relative contribution of galactosylation; and **d** relative con-

tribution of high mannose. Red=ABP, blue=trastuzumab EU, and black=trastuzumab US. ADCC antibody-dependent cellular cytotoxicity

trastuzumab and ABP 980 block downstream signaling and ligand-independent proliferation of HER2-overexpressing tumor cells. Binding to HER2 is mediated by the fragment antigen binding (Fab) region of trastuzumab and ABP 980.

An ELISA was performed to compare the relative binding of ABP 980, trastuzumab (US), and trastuzumab (EU) to HER2. Results are shown in Table 3 and demonstrate that the products have similar HER2 target binding.

### 3.7 Potency: Inhibition of Proliferation in BT-474 cells

Potency was compared between ABP 980 and trastuzumab by measuring their ability to inhibit proliferation of BT-474, a HER2-overexpressing breast carcinoma cell line. Relative potency ranges are shown in Table 3. These results support the conclusion that ABP 980 has similar potency as compared to trastuzumab (US) and trastuzumab (EU).

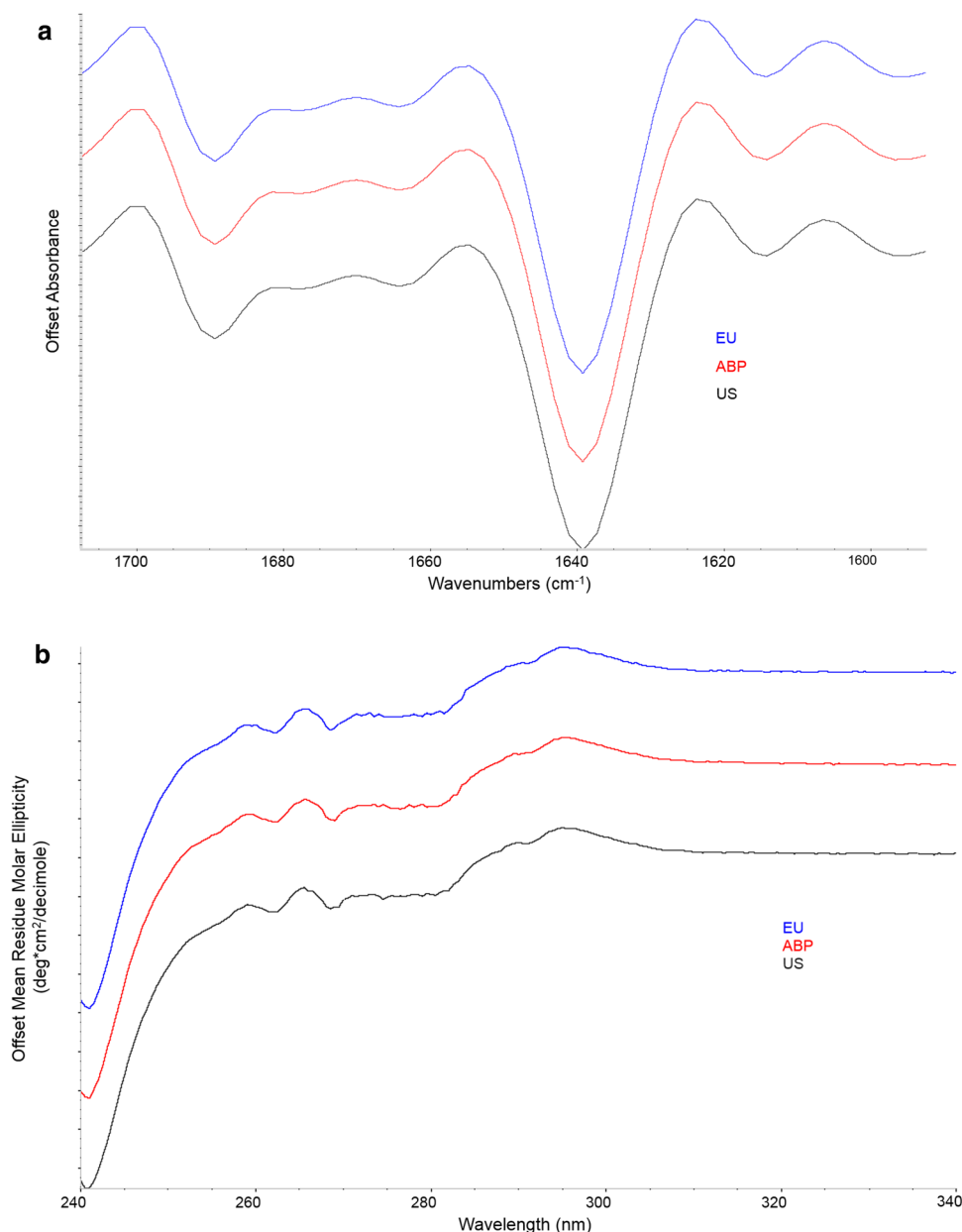
### 3.8 Relative FcRn, FcγRIIa and FcγRIIIa Binding

Trastuzumab and ABP 980 are IgG1 antibodies that bind to multiple FcγRs and the FcRn through their Fc domains. Binding to FcRn has the potential to influence the PK profile of an antibody given its role in serum recycling of IgG, and is thus of interest to evaluate as part of the similarity assessment.

Relative FcRn binding ranges for ABP 980, trastuzumab (US), and trastuzumab (EU) are shown in Table 3. The relative binding ranges of ABP 980, trastuzumab (US), and trastuzumab (EU) demonstrate similar FcRn binding for the three products, supporting the PK equivalence demonstrated in the previously reported PK clinical study, which compared ABP 980 exposure to that of trastuzumab sourced from the US and EU regions [13].

FcγRIIa has the most widespread expression pattern of the FcγRs, expressed on macrophages, dendritic cells, neutrophils, basophils, eosinophils, and platelets. It is a

**Fig. 3** Higher order structure comparisons of trastuzumab (EU) (top, blue line), ABP 980 (middle, red line), and trastuzumab (US) (bottom, black line): **a** Fourier-transformed infrared spectroscopy (FTIR) and **b** near ultraviolet-circular dichroism (UV CD)



low-affinity receptor, interacting primarily with IgG in complexed or aggregated form and plays a role in pathogen clearance through ADCP. Trastuzumab has been reported to exhibit ADCP activity, although the clinical relevance of this effector function has not been determined [6, 16, 17]. Fc $\gamma$ RIIa has two common allelic variations at position 131, histidine (131H) and arginine (131R). The binding affinity for these variants for IgG1 antibodies has been reported to be within 1.5-fold [18]; thus binding to either variant is considered representative. Relative binding ranges to Fc $\gamma$ RIIa (131H) are shown in Table 3 and demonstrate similar binding for the three products.

Fc $\gamma$ RIIIa is a pro-inflammatory Fc $\gamma$ R expressed on effector cells, including natural killer (NK) cells. Fc $\gamma$ RIIIa

mediates ADCC activity, and binding to this receptor is influenced by the glycan profile, specifically the levels of afucosylated, galactosylated, and high mannose species [19–22]. Fc $\gamma$ RIIIa has two allelic variants that have been characterized as the high-affinity variant (158 V) and low-affinity variant (158F) [18]. Relative Fc $\gamma$ RIIIa (158 V) and Fc $\gamma$ RIIIa (158F) binding ranges for ABP 980, trastuzumab (US), and trastuzumab (EU) are shown in Table 3.

Similar to the observations reported in Kim et al. [23], Amgen also observed high variability in Fc $\gamma$ RIIIa binding for a subset of trastuzumab lots that correlated with changes in specific glycans. Overall, ABP 980 exhibits similar binding to both variants of Fc $\gamma$ RIIIa, albeit within a narrower range, as compared to trastuzumab (US) and trastuzumab

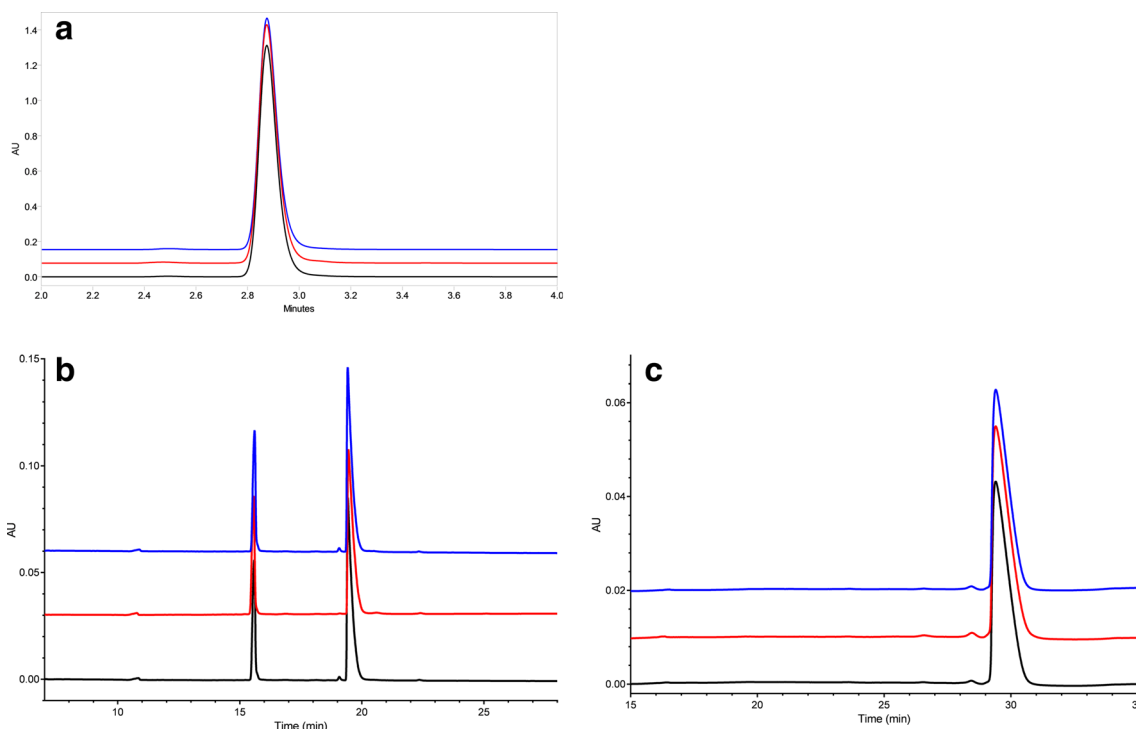


**Fig. 4** Purity comparison of trastuzumab (EU) (top, blue line), ABP 980 (middle, red line), and trastuzumab (US) (bottom, black line): **a** size variant profiles assessed by size-exclusion high-performance

liquid chromatography; **b** size variant profiles assessed by reduced capillary electrophoresis; and **c** size variant profiles assessed by non-reduced capillary electrophoresis

**Table 3** Summary of key functional activities for ABP 980, trastuzumab (US), and trastuzumab (EU)

Key functional activity	ABP 980 Range (n)	Trastuzumab (US) Range (n)	Trastuzumab (EU) Range (n)
Relative inhibition of proliferation in BT-474 (potency) range (%)	96–122 (22)	88–121 (23)	88–124 (33)
HER2 relative binding range (%)	86–109 (22)	90–117 (23)	85–119 (33)
Relative FcRn binding range (%)	93–116 (22)	78–108 (22)	86–106 (33)
Relative FcγRIIa binding range (%)	90–103 (16)	81–106 (13)	85–108 (13)
Relative FcγRIIIa (158 V) binding range (%)	86–112 (22)	48–120 (23)	48–104 (33)
Relative FcγRIIIa (158F) binding range (%)	97–110 (12)	51–105 (14)	51–115 (11)
Relative PBMC ADCC activity range (%)	82–124 (22)	51–115 (23)	35–119 (33)
Relative NK92 ADCC activity range (%)	79–117 (22)	36–106 (23)	46–143 (33)

ADCC antibody-dependent cellular cytotoxicity, *FcγRIIa* Fc gamma receptor type 2a, *FcγRIIIa* Fc gamma receptor type 3a, *FcRn* Fc neonatal receptor, *HER2* human epidermal growth factor receptor 2, *PBMC* peripheral blood mononuclear cells

(EU). Additionally, the FcγRIIIa binding results are consistent with the range of glycan and ADCC activity observed.

### 3.9 Antibody-Dependent Cellular Cytotoxicity

ADCC occurs when an antibody binds to target cells through its Fab domain while the Fc domain simultaneously engages Fc receptors (e.g., FcγRIIIa) on the surface of effector cells. This leads to activation of the effector cell, granule

exocytosis, and target cell death. Trastuzumab has previously been reported to induce ADCC of cells that overexpress HER2, and ADCC activity has been implicated as an important activity in the clinical efficacy of trastuzumab [24].

Two ADCC assays were employed to compare the relative ADCC activity of ABP 980, trastuzumab (US), and trastuzumab (EU): an ADCC assay using PBMC as effector cells and SKBR3 cells as target cells and an ADCC

assay using engineered NK92 effector cells and HCC2218 target cells. There are multiple choices for effector cells used in ADCC methods including primary NK cells, engineered NK92 cells, reporter cell lines, and PBMC. All the choices show strengths and weaknesses [25]. Given that the time period for the functional similarity assessment of ABP 980 spanned close to 5 years, the use of engineered NK92 cells provided a consistent source of effector cells for comparison of results over the entire period of the assessment. PBMCS from healthy donors were also used to evaluate ADCC activity to provide additional information from a more physiologically relevant effector population to mimic the clinical population studied. Trastuzumab has been shown to mediate ADCC using PBMC in early breast cancer patients, metastatic breast cancer patients and healthy subjects [6] to a similar degree, confirming the clinical relevance of a PBMC ADCC assay.

Results are shown in Table 3 and demonstrate that ABP 980 exhibits similar ADCC activity in both assays, albeit within a narrower range, as compared to the variability observed in the trastuzumab reference product. The ADCC activity results are consistent with the wide ranges of glycan and Fc $\gamma$ RIIIa binding observed in the reference product.

## 4 Conclusion

ABP 980 has been developed as a biosimilar to trastuzumab. In this report, sensitive and orthogonal methods were used to assess analytical and functional similarity between ABP 980 and both FDA-licensed trastuzumab and EU-authorized trastuzumab. These studies form part of the totality of evidence and follow the stepwise approach to evaluating biosimilars recommended by the FDA and EMA.

The results of these studies demonstrate that ABP 980 is analytically highly similar to trastuzumab with respect to identity, general properties, primary and higher-order structure, biological activity and carbohydrate structure. Where minor differences are noted, they have been evaluated and found unlikely to impact clinical performance. The totality of evidence, including the recently reported PK and clinical efficacy similarity of ABP 980 [13, 26], further supports that ABP 980 is highly similar to FDA-licensed trastuzumab and EU-authorized trastuzumab.

**Acknowledgements** Thanks to Gwen Maher, Nahira Miscalichi, Shannon Moser, Rupa Padaki, Drew Shami, Junyan Shu and Andrea Treptow for biological characterization support, Cynthia Li, Jie Wen, George Svitel and Nancy Jiao for higher order structure and aggregates and particles support, and Marsha Furtado and Andrew Dykstra for glycan mapping and peptide mapping methods support.

## Compliance with Ethical Standards

**Funding** This study was funded by Amgen Inc.

**Conflict of interest** Katariina M. Hutterer, Alla Polozova, Scott Kuhns, Helen J. McBride, Xingxiang Cao, and Jennifer Liu are employees and stockholders of Amgen Inc.

**Open Access** This article is distributed under the terms of the Creative Commons Attribution-NonCommercial 4.0 International License (<http://creativecommons.org/licenses/by-nc/4.0/>), which permits any noncommercial use, distribution, and reproduction in any medium, provided you give appropriate credit to the original author(s) and the source, provide a link to the Creative Commons license, and indicate if changes were made.

## References

1. Herceptin<sup>®</sup> (trastuzumab) summary of product characteristics, Roche Registration Limited. 2017.
2. Herceptin<sup>®</sup> (trastuzumab) prescribing information, Genentech, a Member of the Roche Group. 2017.
3. Aebi S, Davidson T, Gruber G, Castiglione M, ESMO Guidelines Working Group. Primary breast cancer: ESMO Clinical Practice Guidelines for diagnosis, treatment and follow-up. *Ann Oncol.* 2010;21(Suppl 5):v9–14. <https://doi.org/10.1093/annonc/mdq159>.
4. Cardoso F, Senkus-Konefka E, Fallowfield L, Costa A, Castiglione M. ESMO Guidelines Working Group Locally recurrent or metastatic breast cancer: ESMO Clinical Practice Guidelines for diagnosis, treatment and follow-up. *Ann Oncol.* 2010;21(Suppl 5):v15–9. <https://doi.org/10.1093/annonc/mdq160>.
5. Giordano SH, Temin S, Kirshner JJ, Chandarlapaty S, Crews JR, Davidson NE, Esteva FJ, Gonzalez-Angulo AM, Krop I, Levinson J, Lin NU, Modi S, Patt DA, Perez EA, Perlmutter J, Ramakrishna N, Winer EP, American Society of Clinical Oncology. Systemic therapy for patients with advanced human epidermal growth factor receptor 2-positive breast cancer: American Society of Clinical Oncology clinical practice guideline. *J Clin Oncol.* 2014;32(19):2078–99. <https://doi.org/10.1200/jco.2013.54.0948>.
6. Petricevic B, Laengle J, Singer J, Sachet M, Fazekas J, Steger G, Bartsch R, Jensen-Jarolim E, Bergmann M. Trastuzumab mediates antibody-dependent cell-mediated cytotoxicity and phagocytosis to the same extent in both adjuvant and metastatic HER2/neu breast cancer patients. *J Transl Med.* 2013;11:307.
7. Zelenetz AD, Ahmed I, Braud EL, Cross JD, Davenport-Ennis N, Dickinson BD, Goldberg SE, Gottlieb S, Johnson PE, Lyman GH, Markus R, Matulonis UA, Reinke D, Li EC, DeMartino J, Larsen JK, Hoffman JM. NCCN biosimilars white paper: regulatory, scientific, and patient safety perspectives. *J Natl Compr Cancer Netw.* 2011;9(Suppl 4):S1–22.
8. US Department of Health and Human Services, Food and Drug Administration, Center for Drug Evaluation and Research, Center for Biologics Evaluation and Research. Quality considerations in demonstrating biosimilarity of a therapeutic protein product to a reference product. Guidance for industry. <http://www.fda.gov/downloads/drugs/guidancecomplianceregulatoryinformation/guidances/ucm291134.pdf>. Accessed 7 July 2016.
9. US Department of Health and Human Services, Food and Drug Administration, Center for Drug Evaluation and Research, Center for Biologics Evaluation and Research. Guidance for industry: clinical pharmacology data to support a demonstration of biosimilarity to a reference product. <http://www.fda.gov/downloads/>

- [Drugs/GuidanceComplianceRegulatoryInformation/Guidances/UCM397017.pdf](#). Accessed 25 Feb 2015.
- European Medicines Agency, Committee for Medicinal Products for Human Use. Guideline on similar biological medicinal products containing monoclonal antibodies—non-clinical and clinical issues. [http://www.ema.europa.eu/docs/en\\_GB/document\\_library/Scientific\\_guideline/2012/06/WC500128686.pdf](http://www.ema.europa.eu/docs/en_GB/document_library/Scientific_guideline/2012/06/WC500128686.pdf). Accessed 7 July 2016.
  - US Department of Health and Human Services. Scientific considerations in demonstrating biosimilarity to a reference product. Guidance for industry. <http://www.fda.gov/downloads/Drugs/GuidanceComplianceRegulatoryInformation/Guidances/UCM291128.pdf>. Accessed 7 July 2016.
  - Hanes V, Born T, Chow V, Coon M, Zhang N, Rohrbach A, Crouse-Zeineddini J, Markus R. Functional and human pharmacokinetic similarity of ABP 980 and trastuzumab. In: Poster presented at European Breast Cancer Conference, 2016 Mar 9–11; Amsterdam, the Netherlands.
  - Hanes V, Chow V, Zhang N, Markus R. A randomized, single-blind, single-dose study evaluating the pharmacokinetic equivalence of proposed biosimilar ABP 980 and trastuzumab in healthy male subjects. *Cancer Chemother Pharmacol*. 2017;79(5):881–8. <https://doi.org/10.1007/s00280-017-3286-9>.
  - von Minckwitz G, Ponomarova O, Morales S, Zhang N, Hanes V. Efficacy and safety of biosimilar ABP 980 compared with trastuzumab in HER2 positive early breast cancer. In: European Society for Medical Oncology Annual Meeting, Sept 8–12, Madrid, Spain, (2017) Abstract #151D.
  - Pace N, Vajdos F, Fee L, Grimsley G, Gray T. How to measure and predict the molar absorption coefficient of a protein. *Protein Sci*. 1995;4:2411–23.
  - Lazar GA, Dang W, Karki S, Vafa O, Peng JS, Hyun L, Chan C, Chung HS, Eivazi A, Yoder SC, Vielmetter J, Carmichael DF, Hayes RJ, Dahiyat BI. Engineered antibody Fc variants with enhanced effector function. *Proc Natl Acad Sci*. 2006;103(11):4005–10. <https://doi.org/10.1073/pnas.0508123103>.
  - Jung ST, Kelton W, Kang TH, Ng DTW, Andersen JT, Sandlie I, Sarkar CA, Georgiou G. “Effective phagocytosis of low Her2 tumor cell lines with engineered, aglycosylated IgG displaying high FcγRIIIa affinity and selectivity. *ACS Chem Biol*. 2013;8(2):368–75. <https://doi.org/10.1021/cb300455f>.
  - Bruhns P, Iannascoli B, England P, Mancardi D, Fernandez N, Jorieux S, Daëron M. Specificity and affinity of human Fcγ receptors and their polymorphic variants for human IgG subclasses. *Immunobiology*. 2009;113(16):3716–25. <https://doi.org/10.1182/blood-2008-09-179754>.
  - Jefferis R, Lund J, Pound JD. IgG-Fc-mediated effector functions: molecular definition of interaction sites for effector ligands and the role of glycosylation. *Immunol Rev*. 1998;163:59–76.
  - Houde D, Peng Y, Berkowitz SA, Engen JR. Post-translational modifications differentially affect IgG1 conformation and receptor binding. *Mol Cell Proteom*. 2010;9(8):1716–28. <https://doi.org/10.1074/mcp.M900540-MCP200>.
  - Kumpel BM, Rademacher TW, Rook GA, Williams PJ, Wilson IB. Galactosylation of human IgG monoclonal anti-D produced by EBV-transformed B-lymphoblastoid cell lines is dependent on culture method and affects Fc receptor-mediated functional activity. *Hum Antibodies Hybridomas*. 1994;5(3–4):143–51.
  - Thomann M, Reckermann K, Reusch D, Prasser J, Tejada ML. Fc-galactosylation modulates antibody-dependent cellular cytotoxicity of therapeutic antibodies. *Mol Immunol*. 2016;73:69–75. <https://doi.org/10.1016/j.molimm.2016.03.002>.
  - Kim S, Song J, Park S, Ham S, Paek K, Kang M, Chae Y, Seo H, Kim HC, Flores M. Drifts in ADCC-related quality attributes of Herceptin®: impact on development of a trastuzumab biosimilar. *MAbs*. 2017;9(4):704–14. <https://doi.org/10.1080/19420862.2017.1305530>.
  - Vu T, Claret FX. Trastuzumab: updated mechanisms of action and resistance in breast cancer. *Front Oncol*. 2012;18(2):62. <https://doi.org/10.3389/fonc.2012.00062>.
  - Hsieh YT, Aggarwal P, Cirelli D, Gu L, Surowy T, Mozier NM. Characterization of FcγRIIIa effector cells used in in vitro ADCC bioassay: comparison of primary NK cells with engineered NK-92 and Jurkat T cells. *J Immunol Methods*. 2017. <https://doi.org/10.1016/j.jim.2016.12.002>.
  - von Minckwitz G, Colleoni M, Kolberg HC, Morales S, Santi P, Tomasevic Z, Hanes V. Efficacy and safety of ABP 980 compared with reference product in women with HER2-positive early breast cancer (LILAC study): a randomized, double-blind, phase 3 trial. *Lancet Oncol*. 2018;19(7):987–98. [https://doi.org/10.1016/S1470-2045\(18\)30241-9](https://doi.org/10.1016/S1470-2045(18)30241-9).